Macromolecules

Article

pubs.acs.org/Macromolecules

Synthesis of Main-Chain Poly(fullerene)s from a Sterically Controlled Azomethine Ylide Cycloaddition Polymerization

Hasina H. Ramanitra,[†] Hugo Santos Silva,[†,‡] Bruna A. Bregadiolli,[†,§] Abdel Khoukh,[†] Craig M. S. Combe,[†] Simon A. Dowland,[∥] Didier Bégué,[‡] Carlos F. O. Graeff,[§] Christine Dagron-Lartigau,[†] Andreas Distler,[∥] Graham Morse,[⊥] and Roger C. Hiorns*[,#]

[†]Université de Pau et des Pays de l'Adour, IPREM (EPCP, CNRS-UMR 5254), 2 Avenue Président Angot, 64053 Pau, France

[‡]Université de Pau et des Pays de l'Adour, IPREM (ECP, CNRS-UMR 5254), 2 Avenue Président Angot, 64053 Pau, France

[§]Departamento de Física-FC, UNESP, Av. Luiz Edmundo Carrijo Coube, 14-01, 17033-360 Bauru, Brazil

[∥]Belectric OPV GmbH, Landgrabenstr. 94, 90443 Nürnberg, Germany

[⊥]Merck Chemicals Ltd., Chilworth Technical Centre, University Parkway, SO16 7QD Southampton, United Kingdom

[#]CNRS, IPREM (EPCP, CNRS-UMR 5254), 64053 Pau, France

Supporting Information

ABSTRACT: Fullerene is used as a monomer in this simple method to prepare soluble, well-defined polymers. The sterically controlled azomethine ylide cycloaddition polymerization of fullerene (SACAP) yields macromolecules with molecular weights of around 25 000 g mol^{-1}. Importantly, cumbersome comonomers are employed to restrict cross-linking. Extensive characterizations, with the help of modeling studies, indicate that the polymers are regio-irregular with a majority of *trans*-**3** isomers. Of particular interest is the exceptional ease of preparing polymers with zero metal content.

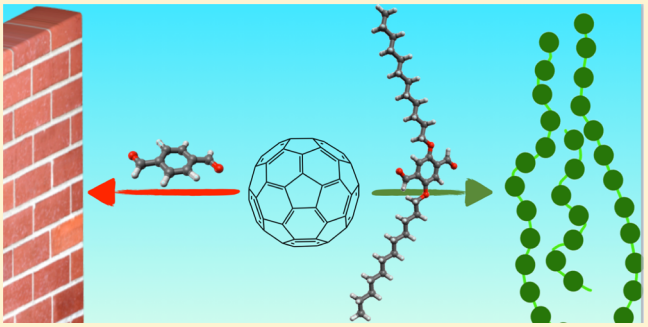

INTRODUCTION

Azomethine ylide cycloadditions to fullerene (C_{60}),[1] commonly called Prato chemistry, by way of their facile nature and adaptability to numerous groups have provided pyrrolidinofullerenes of interest for photovoltaics,[2] organic electronics,[3] medicine,[4−6] and molecular machines.[7] However, due to the difficulties of controlling multiadditions to this spherical molecule combined with its relatively poor reactivity,[8] it has been impossible to our knowledge to form poly(fullerene)s in a controlled manner using this chemistry. While a great challenge, the synthesis of soluble poly(pyrrolidinofullerene)s (PPCs) might extend their optoelectronic and biological properties by combination with the excellent processing, stabilities, and meso-morphology of polymers.[9] While C_{60} is typically incorporated into polymers as a pendent moiety,[10] as it is possible to limit reactions to one site, such materials tend to suffer from C_{60}'s strong tendency to aggregate.[11] A possible route to resolving this is by using C_{60} as a monomer, with highly soluble comonomers, so that the C_{60} is geometrically forced to act like a vector in a linear chain.

More generally speaking, there are numerous challenges to preparing polymers from C_{60}, not least the difficulty of restricting the number of additions to the C_{60} sphere to two when there are 30 [6,6]-bonds. This renders cross-linking reactions probable. While the atom transfer radical addition polymerization (ATRAP) of fullerene permits directed, paired radical additions to one C_{60} phenyl ring at 1,4-positions,[12] it requires high quantities of CuBr which elicits concerns of expense and impact on device operation with even minute residual impurities.[13] Other methods of fullerene polymerization,[10] notably by Diels−Alder chemistry,[14] the use of methano-bridges,[15] or tether-directed premodification of C_{60} with bis(sulfonium ylides)[16] respectively result in cross-linking, intractable products, and the use of complex preparative chemistry.

Successful preparation of PPCs would allow metal-free polymers to be made with facile comonomer modulability for further adaptation to medical and bioelectronic applications and possibly result in materials for use as n-type semiconductors in organic (opto)electronics through pertinent modification of the C_{60} LUMO levels. Usefully, C_{60} bis-adducts typically raise the V_{oc} of photovoltaic devices by ca. 100 mV with respect their monoadduct counterparts due to their higher LUMOs.[17] However, the formation of linear polymers needs high reaction yields (>95%) and exclusive bis-adduct formation. The reaction of C_{60} and azomethine ylides reportedly have

Received: December 29, 2015
Revised: February 7, 2016
Published: February 19, 2016

DOI: 10.1021/acs.macromol.5b02793
Macromolecules 2016, 49, 1681−1691

yields around 80% with respect C_{60} and, when "pushed" beyond monoadduct formation by the addition of excess glycines, give rise to mixtures of bis- and multi-adducts.[1b,18,19] This would result in insoluble, cross-linked polymers.

In any azomethine ylide bis-addition to fullerene, there are eight possible product pyrrolidinofullerene bis-adducts; these addition patterns are shown in Figure S1 of the Supporting Information. Kordatos et al. demonstrated preferential bis-additions occurring at *trans*-**3** and *equatorial* positions and then *trans*-**2**, *trans*-**4**, and *cis*-**2** in that order when reacting C_{60} with cumbersome groups; the order was modified and extended for smaller reagents to *trans*-**3**, *equatorial*, *cis*-**2**, *trans*-**4**, *trans*-**2**, *cis*-**3**, *trans*-**1**, and *cis*-**1**.[20] We found a not dissimilar order (*trans*-**2**, *trans*-**3**) when adding cumbersome polymers to C_{60}, although *cis* and *equatorial* isomers were excluded due to steric constraints.[21] In all cases, tris-adducts have been found, and their presence increases with reaction times. Tris-additions are particularly deleterious to the formation of soluble polymers as even low concentrations would form cross-links. Nevertheless, given the possibility of some control over addition patterns to C_{60}, it was wondered whether the employment of bis-aldehydes with large side groups could lead to linear PPC_{60}s.

This work thus reports the remarkable finding that under sterically controlled conditions, it is possible to prepare highly soluble PPCs with molecular weights greater than 25 000 g mol^{-1} in a one-pot, metal-free, adaptable process. Because of its modularity, it is expected that this new sterically controlled azomethine ylide cycloaddition polymerization (SACAP) might facilitate the formation of a wide range of materials. It is demonstrated here with organic photovoltaic (OPV) cells.

RESULTS AND DISCUSSION

Comonomer Preparation. To explore the possibility of sterically controlling the polymerization, three possible comonomers with increasingly large side groups were chosen and prepared as in Scheme 1: terephthaldehyde (**1**), bis-2,5-(octyloxy)terephthaldehyde (**5**), and bis-2,5-(dodecyl)-terephthaldehyde (**8**). Aromatic-oxy-alkyl side groups are chosen for their expected photostability,[22] high solubility, and ease of preparation via a Williamson condensation of hydroquinone (**1**) with respective alkyl bromides in reasonable yields (60−70%).[23] It was expected that the subsequent bis-bromomethylation might be sensitive to the presence of large alkyl chains; indeed, prior work by Made et al. showed with small substituents yields of around 95% could be obtained,[24] but in our case we had to be content with yields around 75%. Indeed, attempting to make 2,5-bis(bromomethyl)-1,4-bis-(hexadecyl)benzene, we found yields were variable. Furthermore, while the alternate route provided by Wang et al. was found manageable,[23] it required five steps in all from the hydroquinone to the aldehyde aromatic ether **5** or **8**. Therefore, a "short cut" was found by going from the bromomethylated product with slight modification of ref 25. Thus, **5** and **8** were successfully prepared by oxidation with dimethyl sulfoxide, and while low to reasonable yields (21−47%) were found, two synthetic steps had been removed. Full details of the syntheses along with ^1H and ^{13}C NMR can be seen in the Supporting Information (Figures S2−S13).

Formation of PPC1−PPC6. In order to attain high molar masses, it was expected that long reaction times (i.e., ca. 18 h) would be required given the low reactivity of fullerene. As mentioned above, in the presence of excess aldehydes, extended reactions can lead to tris-adducts.[20] Similarly, the use of excess

Scheme 1. Syntheses of the Oligo(pyrrolidinofullerene)s and PPCs[a]

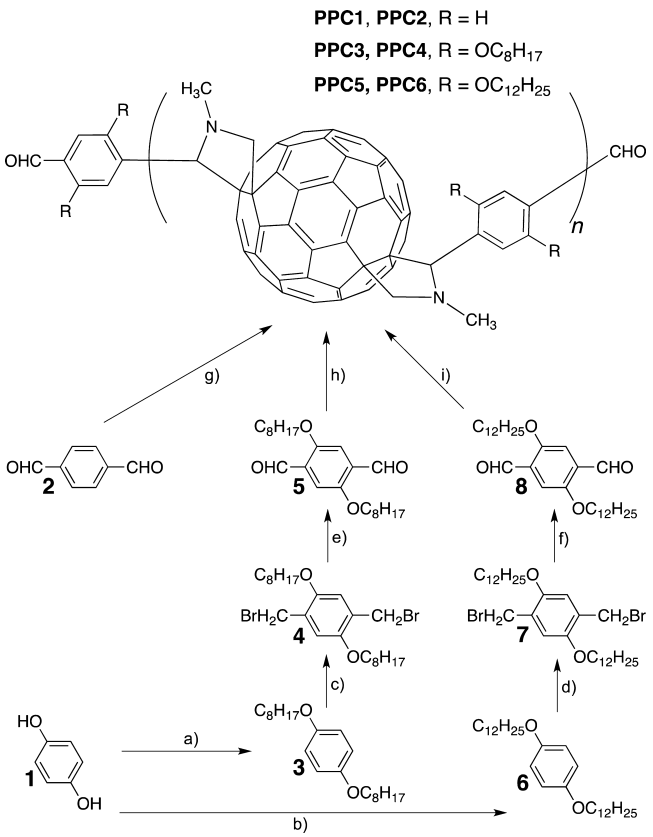

[a]Reagents and conditions: (a) 1-bromooctane, K_2CO_3, **1**, acetonitrile, 70%; (b) 1-bromododecane, K_2CO_3, **1**, acetonitrile, 60%; (c) (-CH_2O-), acetic acid, **3**, HBr, 73%; (d) (-CH_2O-), acetic acid, **6**, HBr, 75%; (e) $NaHCO_3$, **4**, dimethyl sulfoxide, 47%; (f) $NaHCO_3$, **7**, dimethyl sulfoxide, 21%; (g) C_{60}, *N*-methylglycine, **2**, toluene or DCB, respectively, for **PPC1**, 38%, and **PPC2**, 30%; (h) C_{60}, *N*-methylglycine, **5**, toluene or DCB, respectively, for **PPC3**, 41%, and **PPC4**, 58%; (i) C_{60}, *N*-methylglycine, **8**, toluene or DCB, respectively, for **PPC5**, 42%, and **PPC6**, 35%.

N-alkylglycine, while ensuring bis-additions to C_{60}, can also lead to multiadditions.[19] Therefore, to allow long reactions while minimizing multiadditions, so that high molar mass polymers could be formed, the reagents were mixed at absolute ratios, i.e., **2** or **5** or **8**: C_{60}: *N*-methylglycine, respectively, at 1:1:2. Two extreme sets of conditions were employed to better understand the reaction, namely (A) toluene, 110 °C, and ca. C_{60} 0.91 mg toluene mL^{-1} or (B) 1,2-dichlorobenzene (DCB), 150 °C, C_{60} 20 mg DCB mL^{-1}. The concentrations were chosen as the highest possible without risking fullerene precipitation. Full experimental details, and 1D and 2D NMR, are given in the Supporting Information (Figures S14−S35).

The results of size exclusion chromatography (SEC) of **PPC1−PPC6** show an increase in molecular weights with the increasing size of the comonomer chains, whether the reaction is in toluene (Figure 1a) or in DCB (Figure 1b). Figure S36 shows all curves on the same axes. The exceptionally poor solubility of **PPC1** and **PPC2** combined with their low molecular weights and the difficulties of purifications (*vide infra*) confirm high levels of cross-linking. The use of high concentrations of reagents and temperature in method B permitted high yields of soluble long chains with sterically

DOI: 10.1021/acs.macromol.5b02793
Macromolecules 2016, 49, 1681−1691

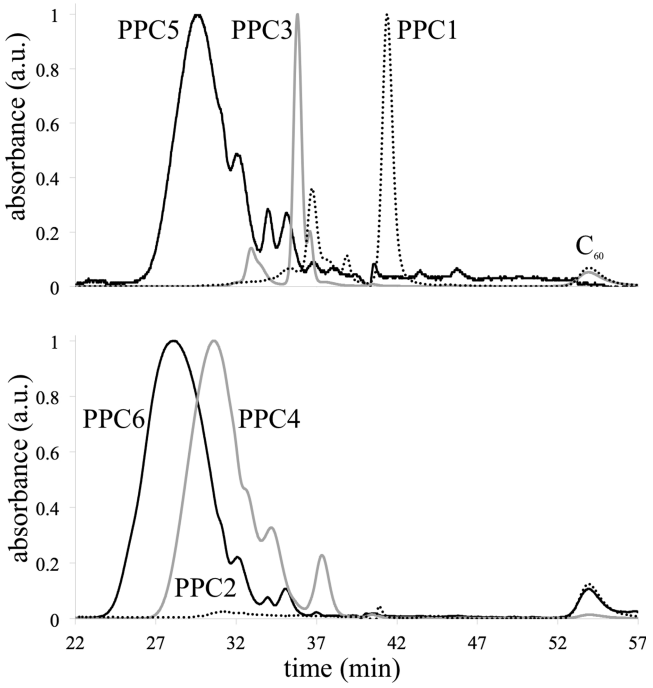

Figure 1. SECs of oligo(pyrrolidinofullerene)s and PPCs (THF, λ = 300 nm): (a) from toluene 110 °C and (b) from DCB at 150 °C.

cumbersome **PPC4** but also led to low yields and cross-linking with **PPC2**. In effect, the use of large comonomers is more critical to high polymer formation under high temperature and concentration conditions.

Table 1 brings together values from SECs shown in Figure 1. Normal polystyrene-based calibration is inadequate for these polymers: C_{60} elutes extremely late from the column, as shown by peaks at ca. 54 min, a full 13 min *after* the toluene marker.[26] Thus, the values in Table 1 severely underestimate the actual value for the molar masses of the polymers. A better, if approximate, estimation is made by inspecting the number of peaks from right to left and assuming that each is due to an integral number of repeating units, in a method that has been successfully employed elsewhere.[12,14] Once discrete peaks are no longer discerned then, by definition, a polymer has been attained.[27] **PPC1** and **PPC2** show weak signals in the column due to their exceptionally low solubility—a strong indicator of their cross-linked nature. Furthermore, their low molar masses, high dispersities, and multimodal curves indicate reactions limited by cross-linking and precipitation. Turning to poly-{fullerene-*alt*-[2,5-bis(octyloxy)terephthalaldehyde]} (**PPC3** and **PPC4**), made with sterically larger comonomers, there is a clear increase in mass, making them respectively around 5850 and 15 200 g mol^{-1} at their M_ps. The former, made in toluene, has a growth inhibited by the low concentration and temperature of the reaction. The low concentration enhances the possibility of the formation of macrocycles,[28] which may also explain the numerous low molecular weight materials. An initial exploration of ring structures was performed in AM1 (Gaussian '09)[29] which tentatively suggested that the ring strain imposed by the bulk of in-chain C_{60} may be overcome when chains are at least five or so repeating units long. **PPC4**, prepared at 150 °C in DCB, demonstrates polymer-like qualities, with the formation of a smooth SEC peak uninterrupted at high molecular weights and only a few lower molecular weight oligomers. While cross-linking cannot yet be ruled out, it is no longer present enough to dominant the solution properties of the material. This effect is further strengthened when considering **PPC5** and **PPC6**, made with the most cumbersome comonomers. The molecular weights obtained from counting off peaks are respectively around 19 100 and 24 300 g mol^{-1}, and the materials show high solubilities.

The SECs show that the choice of the comonomer has a great role in determining the molecular weights of the final products: the greater the bulk of the comonomers, the more effective the blocking of multiple attacks on the fullerene and the reduced number of cross-links. Using high concentrations

Table 1. Molecular Characteristic of the Materials Studied[a]

Polymer	Comonomer	Condition set[a]	M_w[b] (g mol^{-1})	$Đ$[b]	M_p (g mol^{-1}) [repeating units][c]
PPC1	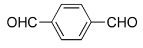	A	820	4.4	900 [1]
PPC2	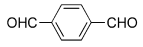	B	1850	9.8	8000 [12]
PPC3	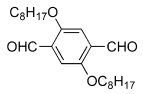	A	3360	1.1	5850 [5]
PPC4	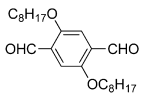	B	4640	2.2	15200 [13]
PPC5	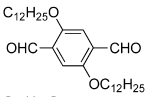	A	4630	1.7	19100 [15]
PPC6	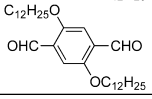	B	10840	1.9	24300 [19]

[a]A = refluxing toluene; B = DCB, 150 °C. [b]SEC (polystyrene standards, THF, 30 °C, UV 300 nm). [c]Most probable M_p by deconvolution of SEC curves.

DOI: 10.1021/acs.macromol.5b02793
Macromolecules 2016, 49, 1681−1691

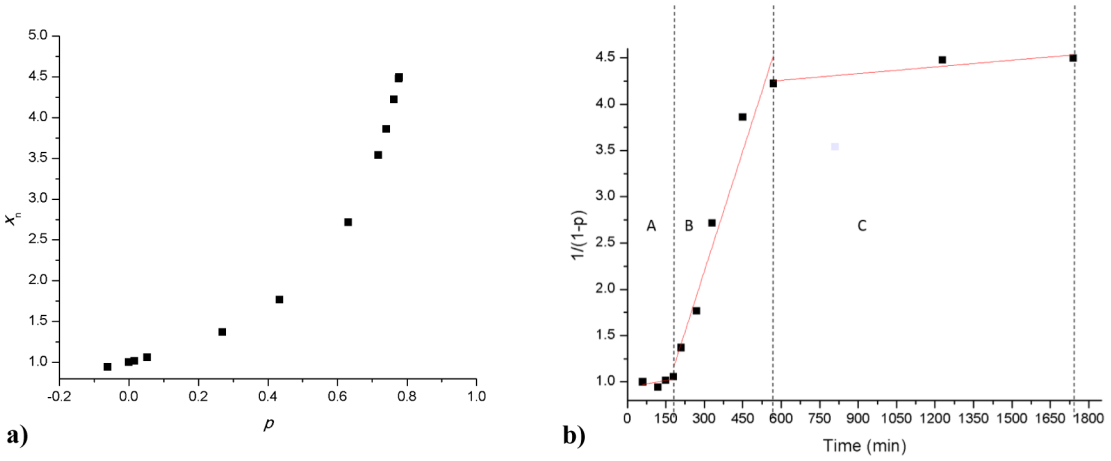

Figure 2. Plots for **PPC4** of (a) the variation in x_n with p for the formation of **PPC4** and (b) of $1/(1 - p)$ against time showing three different regimes (A, B, and C). Straight lines are linear fits within each domain.

and high temperatures can increase the molecular weights. Furthermore, current work has shown that even higher molecular weights are indicated (ca. 70 000 g mol^{-1}) when using chlorinated solvents in the SEC in place of THF; however, these values require verification. MALDI-TOF was attempted but resulted in indeterminate peaks due to secondary, *in situ* reactions.[30]

To better understand the importance of temperature and C_{60} concentration on the reaction, further experiments were performed at fixed, comparable concentrations and temperatures; i.e., the polymerization was performed using **5** in DCB at both 110 and 150 °C, with either 0.9 or 20 mg mL^{-1} of C_{60}. As shown in the Supporting Information (Figures S37 and S38), the results are much as those expected. Both temperature and concentration result in increased molar masses for a fixed reaction time; however, temperature clearly causes the greater effect. The ylide cycloaddition is known to require high temperatures.[31] Interestingly, when performed at the lower temperature, the dispersity ($Đ = M_n/M_w$)[32] of the product is very high ($Đ > 30$). As to why this is happening is not clear and will be considered in future studies. To sum for now, performing the reaction at 150 °C with a concentration of 20 mg mL^{-1} results in PPCs with reasonably high molecular weights and low dispersities.

Kinetics. Given the mechanism of the cycloaddition to C_{60},[1] it was expected that the formation of macromolecules would be essentially in accordance with step polymerization kinetics[9] modified by aggregation effects, steric constraints, or precipitation. To investigate, the formation of **PPC4** in DCB (150 °C, C_{60} at 20 mg mL^{-1}) was followed by SEC, as shown in Figure S39. The values of M_w, M_n, and $Đ$ are given in the Supporting Information (Table S1). Even though the values for M_n are clearly erroneous due to retention of polymers, oligomers, and C_{60} in the column, the data can be explored when assuming it to be a self-consistent set. Figure S40a shows that M_n does not increase linearly with time; it initially decreases. This is most likely due to the dissolution of reagents with time—aggregates of C_{60} disappearing over a period of an hour or so. Indeed, this is further confirmed when considering the reaction in terms of the consumption of C_{60}, as in Figure S40b. There is an initial increase in C_{60} concentration due to the delay in its dissolution; it is still in aggregates that are filtered out prior to injection in the machine. There then follows a phase of about 3 h where there is a negligible increase in M_n due to a formation of either or both ylides and low molecular weight oligomers.

Assuming that the second part of the reaction, between ca. 180 and 600 min, is a second-order polyaddition (other order plots did not give better results) between that of the ylide and C_{60}, and given that the average degree of polymerization (x_n) is related to the extent of the reaction (p) through the Carothers equation, i.e., $x_n = 1/(1 - p)$,[33,34] the polymerization can be better understood as a function of its progress, as detailed in Table S2 and shown in Figure 2a. The typical curve for a polyaddition is obtained; however, it falls well short of $p = 1$, i.e., a complete reaction. Toward the end of the reaction, for a pure polyaddition one would expect $Đ = 2$ (obtained from the Flory equation, $Đ = 1 + p$); however, actual values upward of 5 are obtained (listed in Table S3). This difference would tend to confirm that aggregation occurs at high molecular weights but may also confirm the formation of macrocyclics.[28]

Again, making the assumption that the main part of the polymerization is a second-order step polymerization by plotting $1/(1 - p)$ against time (Figure 2b), an indication of the rate constant (k) during the reaction can be found in accordance with $[M]_0kt = 1/(1 - p) - 1$ where $[M]_0$ is the initial concentration of C_{60}.[33,34] Confirming the prior results, Figure 2b shows three distinct regimes: (A) a period of induction, where C_{60} dissolution or ylide formation or both are rate determining up to the 180th minute; (B) a period where the polymerization proceeds in accordance with a typical step growth reaction to around 10 h; (C) where the polymerization is limited by product precipitation. For each region, the value of the rate constants have been calculated and are shown in Table S4. $[M]_0$ is assumed to be the initial C_{60} concentration. As possible macrocyclic formation is not taken into account, such values should be considered an initial estimate only. For regime B, k is of the order of 7.1×10^{-4} L mol^{-1} s^{-1}, nearly 3 times the rate constant (2.9×10^{-4} L mol^{-1} s^{-1}) for the induction period in regime A. The final domain C gives a rate constant of around 4.5×10^{-4} L mol^{-1} s^{-1} and is most likely slowed by precipitation. The possibility of retro-cycloadditions cannot be completely excluded; however, for them to occur we would expect that any degradation products, i.e., azomethine ylides, would carry stabilizing substituents such as ester or aryl groups.[35] Indeed, we found by ^{1}H NMR that **PPC4** showed no degradation after 14 h at 150 °C in 1,4-dichlorobenzene-d_4.

DOI: 10.1021/acs.macromol.5b02793
Macromolecules 2016, 49, 1681−1691

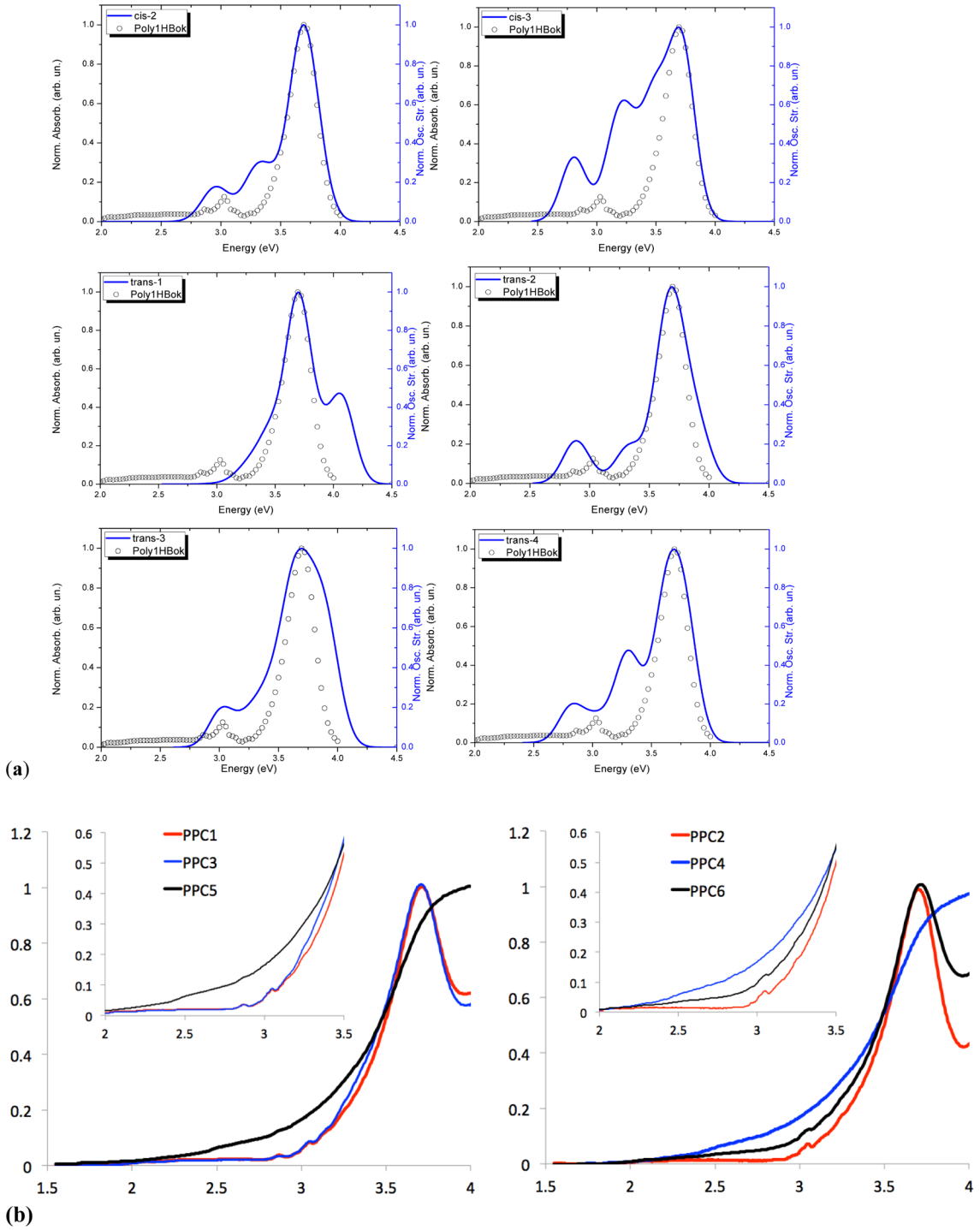

Figure 3. Top: (a) comparisons between the spectra for the generic compound of Figure S41 and **PPC3**. Bottom: (b) comparisons of UV curves (left) **PPC1**, **PPC3**, and **PPC5** and (right) **PPC2**, **PPC4**, and **PPC6** (toluene).

Purification. The removal of C_{60} from macromolecules can be troublesome.[12] While Soxhlet treatment with hexane can leave traces of C_{60} in the product, and five reprecipitations from chlorobenzene into hexane are preferred to remove all traces of C_{60},[36] we felt that this intensive manipulation risked invoking chain cross-linking through oxygen-bridge formation with air[37] and 2 + 2 cycloadditions with light.[38] It was therefore preferable to work with minor concentrations of fullerene in the mixtures, estimated from integration over SECs performed at 300 nm to be of the order of 3 mol % for **PPC1**, **PPC3**, **PPC4**, and **PPC6**. Indeed, using Soxhlet alone, we managed to remove all C_{60} from **PPC5**. ^{13}C NMR (see figures in the Supporting Information), while not quantitative, confirm the scale of these values. However, **PPC2**, could not be washed of its C_{60} which remained of the order of 47 mol %, confirming extremely high levels of cross-linking.

Modeling and UV−Vis Characterization. Given the polymeric nature of the products, it was expected that both UV−vis and NMR characterizations would be complicated by the variety of possible in-chain isomers and the multiplicity of

DOI: 10.1021/acs.macromol.5b02793
Macromolecules 2016, 49, 1681−1691

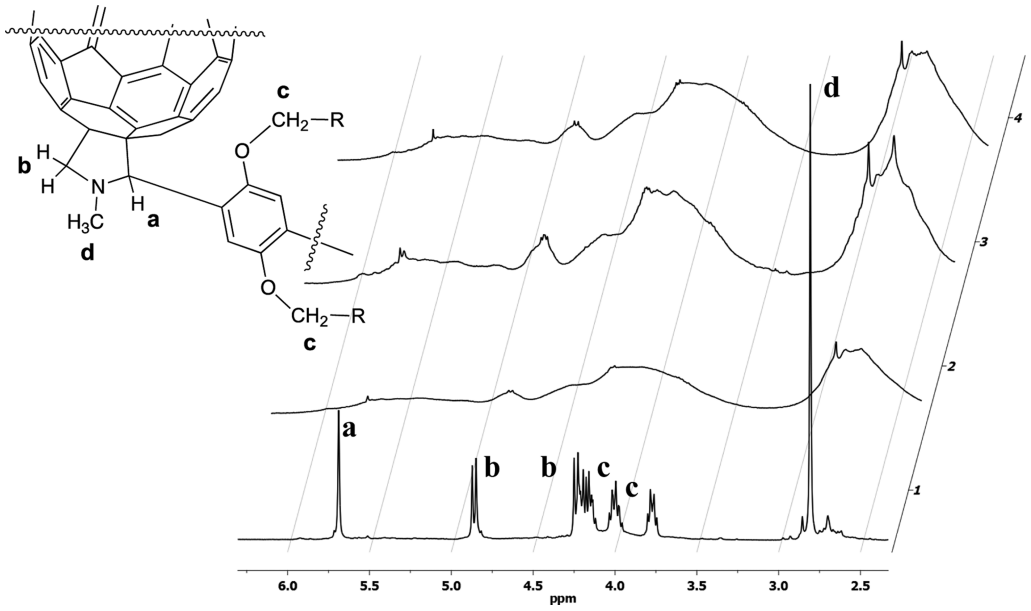

Figure 4. From bottom to top: the ^{1}H spectra (1,4-DCB-d_4) of **PPC3**, **PPC4**, **PPC5**, and **PPC6**.

environments for each repeating unit. Furthermore, UV−vis spectra were not expected to give diagnostic information due to the admixing of multiple absorptions. As mentioned above, a mixture of predominantly *trans*-**3**, *equatorial*, *trans*-**2**, *trans*-**4**, and *cis*-**2** isomers would be expected in the polymer chains.[20,21] *Cis* isomers are generally excluded by steric effects. Modeling was thus explored to determine: first, what UV spectra might be expected for the possible isomers and, second, the most preferred isomer formed by the reaction.

The geometries were optimized within the B3LYP/6-31G** level of theory,[39] and their UV−visible electronic transitions were calculated by time-dependent density functional theory within the same formalism. For all the calculations, the RIJCOSX approximation was used, and all the calculations were run in Orca 3.0.2 software.[40] The theoretical electronic transitions were enveloped by Gaussian functions with 0.125 eV at fwhm and shifted to have their highest-intensity maximum coincident with the experimental spectra. Further experimental notes are given in Figure S41. The calculated curves are exemplified by their comparison against **PPC3** in Figure 3a. The closest correlation between the UV−vis spectrum and the calculated spectra is found with the *trans*-**3** isomer; however, there is also a minor "bump" at ca. 2.8 eV associated with the *trans*-**2** adduct, indicating a mixture of both in the chains and in agreement with prior work,[20] and *trans*-**4** and *equatorial* products appear limited, again in a not unexpected result.[21] Interestingly, when comparing **PPC1**, **PPC3**, and **PPC5** in Figure 3b, the three materials made in toluene, the bump at 2.8 eV is still present, if reduced by the scattering caused by aggregation of **PPC5** and possible steric effects of the larger comonomer. Turning to **PPC2**, **PPC4**, and **PPC6**, the products of reactions in DCB at a higher temperature, the 2.8 eV bump is no longer distinguishable, suggesting that *trans*-**2** additions are reduced. The experiments were numerously repeated and even with ultrasound treatment and purifications, **PPC4** and **PPC5** always gave scattering in the UV−vis spectra, indicting the presence of aggregates. This will be the subject of future studies. In all cases, the correlations between calculated and actual values is poor in the zone below 2.5 eV. In **PPC1** this effect is highly exaggerated (see Figure S42, Supporting Information) and likely due to numerous isomers and tris-adducts.[41]

In an attempt to better understand the underlying process, the frontier molecular orbital-based mechanism of the 1,3-dipolar azomethine cycloaddition to C_{60} was considered. As a pericyclic reaction, Woodward−Hoffmann rules are followed and the frontier molecular orbitals of the 1,3-dipole and the dipolarophile overlap in allowed symmetry of π^4s + π^2s. Such orbital overlaps can be achieved in three ways: type I, II, and III. The dominant pathway is the one which possesses the smallest HOMO−LUMO energy gap.[42] The C_{60} dipolarophile possesses a LUMO, and therefore the orbital overlap occurs between the HOMO of the 1,3-dipole and the LUMO of the already modified C_{60} (i.e., C_{60}-monoadduct). Figure S43 shows the energy diagram in which the HOMO−LUMO gap for two possible configurations, indicated as blue and red, are 4.54 eV and only 0.43 eV, respectively. Thus, any specific reaction site is not ruled out by the C_{60} HOMO but rather by its LUMO. Based on this analysis, and the information garnered from Figure S44 showing frontier orbitals, it is clear that *equatorial* and *trans*-**1** bis-adducts are not favored due to poor LUMO distributions. *Cis*-**1** and *cis*-**2** may occur but suffer from steric hindrance. *Cis*-**3** and *trans*-**4** may also occur but from TDDFT calculations are not apparent. In complete agreement with the above UV−vis work, *trans*-**3** and *trans*-**2** show the most favorable LUMO distributions, while the overall order found is *trans*-**3** > *trans*-**2** > *cis*-**2**/*trans*-**4**/*cis*-**3** > *equatorial*/*trans*-**1** ≫ *cis*-**1**. These results are not unfavorable in comparison with those of Kordatos et al.[20] although they found a greater presence of equatorial materials than we would expect, perhaps due to the different nature of their adduct and the conditions of the reaction.

^{1}H, ^{13}C, and 2-D NMR. All comonomers and polymers were thoroughly characterized by ^{1}H and ^{13}C NMR; polymers were also treated to HMQC and HSQC 2D NMR characterizations. Nevertheless, **PPC1** was not of a high enough solubility to gain complete spectra even when employing 1,4-dichlorobenzene-d_4 at 85 °C. This was due to cross-linking, as confirmed by the presence of trapped fullerene and hexane in well-washed and dried samples and observed in the spectra

DOI: 10.1021/acs.macromol.5b02793
Macromolecules 2016, 49, 1681−1691

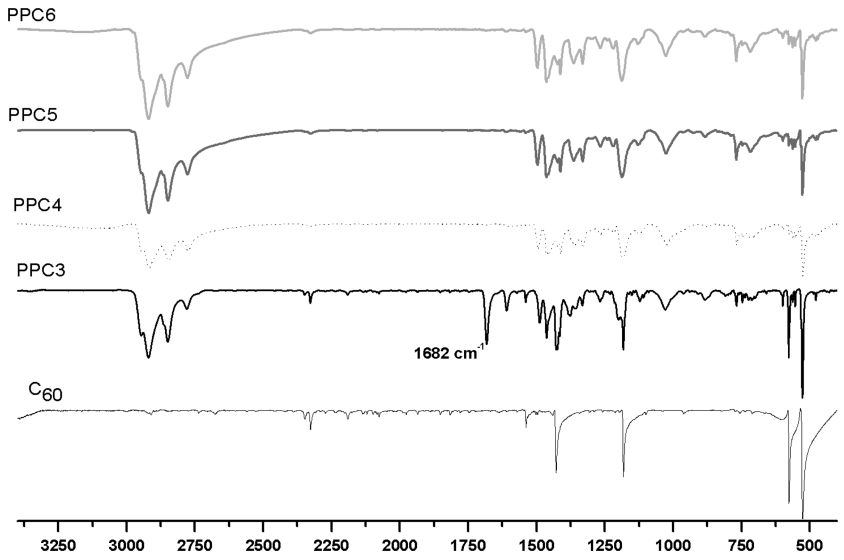

Figure 5. FT-IR characterizations of **PPC3**, **PPC4**, **PPC5**, **PPC6**, and C_{60}.

(Figures S14–S16). In the soluble parts of **PPC1** samples, pyrrolidine adducts were found by way of double–doublets centered at 4.50 ppm (4.14 and 4.85 ppm) due to pyrrolidine methylenes, a singlet at 4.5 ppm from pyrrolidine methines, and a singlet at 2.3 ppm of amino methyl groups. While the ^{1}H NMR of **PPC1** showed two aldehyde peaks, the HSQC NMR (Figure S17) uncovered three at 9.57, 9.52, and 9.45 ppm. The ^{13}C NMR showed three peaks (one a shoulder to the other at 189.9 and 190.0 ppm, respectively) and one very weak peak (189.7 ppm) discerned by adding comonomer as an impurity (Figure S18). This suggested that the mixture contained symmetrical bis-adducts, tris-adducts, and comonomer. **PPC2** could not be characterized as it was insoluble; the higher reaction temperature permitted an even greater level of cross-linking than that found for **PPC1**.

Turning to **PPC3**, the ^{1}H NMR in Figure S19 shows more soluble well-defined samples, indicating reduced cross-linking and less tris-adduct formation. The aldehydes form a large singlet at 10.67. A ^{13}C NMR of the crude sample (Figure S21) and the starting material **5** indicated that one peak was due to a comonomer impurity, while the other, carrying no shoulder, was due to single type of CHO group on the **PPC3**, confirming that the product was mostly made of symmetrical bis-adducts. Figure 4 shows a zoom in the range 6–2.5 ppm wherein the $-N-CH_3$ peaks (2.8–3.0 ppm) show one major peak due to the *trans*-**3** adduct and several minor peaks, probably due to the aforementioned *trans*-**2** and other isomers. Peaks associated with pyrrolidinone groups are labeled in Figure 4. The **PPC3** HSQC NMR (Figure S22) correlations confirmed pyrrolidinones with methylene double doublets at 4.3 and 4.9 ppm, a methine singlet at 5.8 ppm, and an amino methyl singlet at 1.6 ppm. Remarkably, there are multiplet correlations at 4.2, 4.1, and 3.8 ppm (^{1}H) arising from the asymmetry in the $O-CH_2-C_6H_{13}$ side chains of these short oligomeric species.

In the ^{13}C NMR of **PPC3** (Figure S20) more than 30 resonances are present in the region between 133 and 158 ppm. This is due to a mixture of fullerene derivatives with various symmetries. The four resonances around 70 and 76 ppm are characteristic for pyrrolidine sp^3 carbons and confirm the presence of at least two different adducts. These results are in agreement with the UV–vis spectra which indicate the presence of *trans*-**3** and *trans*-**2** bis-adducts (C_2 symmetry), together with the minor *trans*-**4** and *equatorial* bis-adducts (C_s symmetry).[43] Variations in ^{13}C asymmetries (Figure S45b) appear to decrease going up through the sample series (reduction in the peak at ca. 76.7 ppm) and tentatively confirm increased selectivity with increasing adduct size.

As one goes up through the series from **PPC3** to **PPC6**, the increase in the polymeric character of the materials is clearly shown through the peak broadening of the ^{1}H NMR in Figure 4. There is a similar change in all the ^{1}H, ^{13}C, and HSQC spectra (Figures S14–S35 and S45). Given that the SEC values for molar masses were either inaccurate or estimated from peaks, NMR was used to give a more exact estimate of the degree of polymerization (DP_n) and the M_n. Assuming that all chains carried on average one aldehyde group and one C_{60} at the chain-ends, as would be expected for a polyaddition, and that each repeating unit contained two phenylic and six alkyl methylic protons, the DP_n was calculated as a ratio of proton integrals in accordance with eq 1:

$$DP_n = \frac{[\int(\text{phenyl}/2) + \int(\text{methyl}/6)]}{\int \text{CHO}} \quad (1)$$

PPC3 and **PPC5** gave masses of 3600 g mol^{-1} (DP_n = 2.4) and 26 900 g mol^{-1} (DP_n = 21), respectively. The former value confirms that the material is essential low molecular weight oligomers, with the aforementioned asymmetries probably arising through midchain and chain-end groups, whereas **PPC5** shows a strong polymeric character. However, it should be noted that the molecular weights calculated by NMR may contain errors arising from the presence of macrocycles and tris-adducts. Peak estimations, however, tend to underestimate molecular weights due to visual inspection missing peaks. The "real" values are nevertheless, most likely closest to those found by peak inspection, and the data confirm how PS standards can lead to extremely underestimated values for high polymers made from C_{60}. **PPC4** and **PPC6** did not carry identifiable –CHO groups due to either cyclization or the presence of excess C_{60}.

FT-IR Characterization. FT-IR spectra of **PPC3**, **PPC4**, **PPC5**, and **PPC6** shown in Figure 5 confirm the polymeric structures and are consistent with literature values for

DOI: 10.1021/acs.macromol.5b02793
Macromolecules 2016, 49, 1681–1691

comparable, small molecule systems.[44] Absorption bands at 1428, 1182, 576, and 526 cm^{-1} are present in all materials and are attributed to C_{60} vibrations.[45] In the **PPC3** spectrum the contribution of C_{60} is strong, confirming its presence as an impurity; the band C═O stretching band at 1682 cm^{-1} for the aldehyde functions also confirms the relatively low molecular weight of **PPC3**. The vibrational spectra of the compounds confirms their general, similar structures. Going from **PPC3** to **PPC6** peaks between 2500 and 3000 cm^{-1} become stronger and broader, confirming both the higher percentage of alkyl chains in the macromolecules and the materials' increasingly polymeric nature; these bands are due to symmetric and asymmetric stretching of C−H groups and out-of-plane C−H bending at aromatic rings and pyrrolidine groups. The absorption bands for the corresponding bendings participate in the more complex features between 1100 and 1500 cm^{-1}: the presence of alkyl aryl ethers is confirmed by the bands at 1025 cm^{-1}, characteristic of C−O−C group stretching. Absorption bands due to the asymmetric stretching of this group are hidden by absorptions due to fullerene in the region 1200−1275 cm^{-1}.

Thermogravimetric Characterization. Pyrrolidinofullerenes are considered thermally stable and are normally only cleaved when mixed with large excesses of dipolarophiles such as C_{60}.[35a] The thermogravimetric characterizations of **PPC1**−**PPC6** could thus be used to follow the gradual changes in properties while going through the series. For **PPC1**, in Figure S46, there are four steps of decomposition, starting at ca. 120, ca. 250, 350, and 500 °C; **PPC2**, in Figure S47, shows a less pronounced but similar multistep process starting at ca. 135, 250, 350, and 500 °C. The lowest temperature for both samples, respectively 120 and 135 °C, are due to the loss of trapped solvents and reagents. This confirms that **PPC2** is more cross-linked than **PPC1**; the impurities are more strongly trapped in the matrices. The polymers **PPC3**−**6** show a higher thermal stability with a decomposition temperature from around 350 to 400 °C and a loss of around 20% weight in all cases (Figures S48 and S49). These values indicates that it is the alkyl side chains which are lost first in this process. Interestingly, **PPC4** has a slightly higher degradation temperature than the other samples which may point to a better crystallization of this material.

DSC characterizations of **PPC3**, **PPC4**, **PPC5**, and **PPC6** were performed up to 180 °C. Figures S52−S56 show complete first and second heating and cooling passages. After solvents were removed from **PPC1** at ca. 120 °C, there is a featureless curve, indicative of an unstructured material. Indeed, all samples gave featureless curves on their second passages, a not unexpected result for materials containing such cumbersome groups.[9] In all cases, minor transitions were observed around 120−130 °C on the first passage. While these are most likely due to solvents being removed, the possibility that these are arising from disorder−order transitions cannot be excluded. Of these transitions the most remarkable is the endothermic transition of **PPC4** in Figure S54 at 128 °C (Δ_H = 0.26 J g^{-1}) which may result from a reorganization of the polymer.

Photovoltaic Characterization. Functionalized fullerenes have been utilized extensively in the field of organic photovoltaics as an acceptor of charge in the active layers of two-component blend systems.[1b] However, OPVs exploiting polymer−polymer systems with SACAP fullerenes have not yet been reported. Here, for the first time, photovoltaic devices were fabricated incorporating PPCs, **PPC2**, **PPC4**, and **PPC6**, as the accepting species in a blend system (0.8:1 weight ratio) with the well-known organic semiconductor poly(3-hexylthiophene-2,5-diyl) (P3HT).[46] The low power conversion efficiencies (PCEs) achieved are attributed to the devices being processed from industrially applicable xylene under air. The device performances achieved and representative current density−voltage curves are shown in Figure 6. Average PCEs

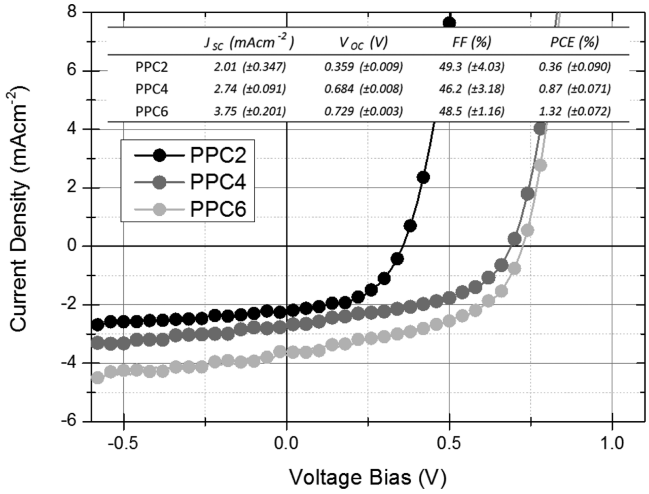

Figure 6. Current−voltage characteristics of a typical photovoltaic device, utilizing an active layer of **PPC2**, **PPC4**, or **PPC6** (black, gray, and light gray circles, respectively) mixed with P3HT, under illumination at ∼100 mW cm^{-2}. Inset: table displaying averages and standard deviations for key solar cell parameters over a set of 11, 13, and 14 devices for **PPC2**, **PPC4**, and **PPC6**, respectively.

obtained for P3HT blends incorporating **PPC2**, **PPC4**, and **PPC6** were 0.36%, 0.87%, and 1.32%, respectively. While relatively low currents and fill factor were obtained, devices (with aliphatic side chains) achieved a high open circuit voltage of around 700 mV consistent with the double functionalization of the fullerene cage.[17] Furthermore, a clear trend in increasing efficiency is observed with increasing poly(fullerene) side chain length. This stands as a proof of concept and is suggestive of the great potential of this class of acceptor to be further improved through facile structural modification. It should be noted that the focus of this work, however, is on the synthesis and demonstration of these materials as a new class of fullerene acceptors. Thus, thorough investigation of the properties of these systems in OPV will be reported on, separately, in due course.

■ CONCLUSION

It has been demonstrated that it is possible to prepare high molecular weight poly(fullerene)s with azomethine ylide cycloadditions, so-called Prato chemistry, when employing sterically cumbersome comonomers to reduce cross-linking. This sterically controlled azomethine ylide cycloaddition polymerization of fullerene (SACAP) results in high polymers with reasonably good solubilities in a number of solvents. The isomeric nature of the polymers is as expected, mixed, however, *trans*-**3** bis-additions are a major component. Of particular interest are the promising photovoltaic properties of these materials which exhibit relatively high V_{oc}s and may have other interesting properties; this will be the focus of forthcoming papers.

DOI: 10.1021/acs.macromol.5b02793
Macromolecules 2016, 49, 1681−1691

EXPERIMENTAL SECTION

A brief, representative synthesis of **PPC5** is given here. All others are given in the Supporting Information. C_{60} (0.05 g, 6.94×10^{-5} mol), **8** (0.035 g, 6.96×10^{-5} mol), and *N*-methylglycine (0.0124 g, 1.39×10^{-4} mol) were dissolved in toluene (55.5 mL) under strictly dry and oxygen-free conditions and heated at reflux for 18 h. The polymer was recovered by precipitation in methanol, filtration through a Soxhlet filter, and a 4 day Soxhlet treatment with hexane. The crude product was dried under reduced pressure to yield 0.038 g (42.3%) of a shiny black powder. SEC, THF eluent at 1 mL min^{-1}, 30 °C, UV = 300 nm: M_n = 2770 g mol^{-1}; mp = 4260 g mol^{-1}; $Đ$ = 1.7.

^{1}H NMR (400.6 MHz, 1,4-DCB-d_4, 85 °C): δ = 0.86 (broad, $-OCH_2(CH_2)_{10}CH_3$), 1.25–2.12 (broad, $-OCH_2(CH_2)_{10}CH_3$), 2.66–2.82 (broad, $-N-CH_3$), 3.39–4.80 (m, broad, $-OCH_2(CH_2)_{10}CH_3$), $-CH_2-N-$), 5.68 (broad, $-CH-N-$), 7.50–7.82 (broad, *aromatics*).

^{13}C NMR (100.16 MHz, 1,4-DCB-d_4, 85 °C): δ = 13.51 (s, $O-CH_2(CH_2)_{10}CH_3$), 22.25 (s, $O-CH_2(CH_2)_9CH_2CH_3$), 25.90 (s, $O-CH_2CH_2CH_2(CH_2)_8CH_3$), 28.97–29.34 (m, $O-CH_2CH_2CH_2-(CH_2)_6CH_2CH_2CH_3$), 31.52 (s, $O-CH_2(CH_2)_8CH_2CH_2CH_3$), 39.26 (s, $-CH_3-N-$), 69.08 (broad, $O-CH_2(CH_2)_{10}CH_3$), 75.37 (broad, $-CH-N-$), 114.56 (broad, *aromatic*), 135.83–147.62 (m, *aromatic, C_{60}*), 152.51 ppm (broad, *aromatic*$-OC_{12}H_{25}$).

2D-HMQC NMR (1,4-DCB-d_4, 85 °C), d = δ = 0.86, 13.51 ($-OCH_2(CH_2)_{10}CH_3$); 1.25–2.12, 22.25–31.52 ($-OCH_2(CH_2)_{10}CH_3$); 2.82, 39.26 ($-N-CH_3$), 3.39–4.80, 69.08 ($-OCH_2(CH_2)_{10}CH_3$), $-CH_2-N-$); 5.68, 75.37 ($-CH-N-$), 7.50–7.82, 114.56 ppm (*aromatics*).

Devices were constructed with the following architecture: ITO/ZnO/photoactive layer/PEDOT:PSS/Ag. ITO was prepared on a flexible PET substrate by sonication in acetone and isopropanol. The active layer solution was prepared by mixing P3HT (Merck Chemicals) and PPC4 in xylene (15:12 mg mL^{-1}) and stirring overnight in an inert atmosphere at 80 °C. ZnO (IBUtec) was deposited directly onto the ITO from a 5 wt % nanoparticle suspension and thermally annealed at 140 °C in air. The active layer and PEDOT:PSS (Heraeus) were then sequentially deposited over the substrate. All aforementioned depositions were carried out with a doctor blade. Electrode deposition was carried out by thermal evaporation of silver under vacuum to produce complete solar cells with active areas of 27 mm^2. Current–voltage characteristics were measured under nitrogen using a Keithley 2400 source meter and a xenon arc lamp with an intensity of approximately 100 mW cm^{-2}.

ASSOCIATED CONTENT

Supporting Information

The Supporting Information is available free of charge on the ACS Publications website at DOI: 10.1021/acs.macromol.5b02793.

Syntheses in whole with NMR and SEC data, kinetic data, modeling results and equipment used (PDF)

AUTHOR INFORMATION

Corresponding Author

*E-mail: roger.hiorns@univ-pau.fr (R.C.H.).

Author Contributions

H.H.R., H.S.S., B.A.B., and C.M.S.C. prepared comonomers. H.H.R. prepared polymers. A.K. performed NMR characterizations. G.M. and S.A.S. prepared devices and characterizations. H.S.S. and D.B. performed modeling experiments. H.H.R., H.S.S., D.B., C.F.O.G., C.D.L., A.D., G.M., and R.C.H. designed the experiments and prepared the manuscript.

Notes

The authors declare no competing financial interest.

ACKNOWLEDGMENTS

Mrs. Meera Stephen is gratefully thanked for her assistance in preparing thin films. Dr. M. Pédeutour is warmly thanked for her administrative support. The research leading to these results has received funding from the French Region Aquitaine under the grant agreement FULLINC 2011 and from European Union Seventh Framework Program (FP7/2011) under grant agreement ESTABLIS no. 290022. B.A.B. gratefully acknowledges FAPESP (2011/02205-3) and CAPES (BEX 11216-12-3) for financial support.

REFERENCES

(1) (a) Maggini, M.; Scorrano, G.; Prato, M. Addition of azomethine ylides to C_{60}: synthesis, characterization, and functionalization of fullerene pyrrolidines. *J. Am. Chem. Soc.* **1993**, *115*, 9798. (b) Prato, M.; Maggini, M. Fulleropyrrolidines: A Family of Full-Fledged Fullerene Derivatives. *Acc. Chem. Res.* **1998**, *31* (9), 519.

(2) (a) Thompson, B. C.; Fréchet, J. M. J. Polymer–Fullerene Composite Solar Cells. *Angew. Chem., Int. Ed.* **2008**, *47*, 58. (b) Kim, H.; Seo, J. H.; Park, E. Y.; Kim, T.-D.; Lee, K.; Lee, K.-S.; Cho, S.; Heeger, A. J. Increased open-circuit voltage in bulk-heterojunction solar cells using a C_{60} derivative. *Appl. Phys. Lett.* **2010**, *97*, 193309. (c) Segura, J. L.; Martín, N.; Guldi, D. M. Materials for organic solar cells: the C_{60}/π-conjugated oligomer approach. *Chem. Soc. Rev.* **2005**, *34*, 31. (d) Delgado, J. L.; Bouit, P.-A.; Filippone, S.; Herranz, M.; Martín, N. Organic photovoltaics: a chemical approach. *Chem. Commun.* **2010**, *46*, 4853. (e) Segura, J.; Giacalone, F.; Gomez, R.; Martín, N.; Guldi, D.; Luo, C.; Swartz, A.; Riedel, I.; Chirvase, D.; Parisi, J. Design, synthesis and photovoltaic properties of [60]fullerene based molecular materials. *Mater. Sci. Eng., C* **2005**, *25*, 835. (f) Topham, P. D.; Parnell, A. J.; Hiorns, R. C. Block copolymer strategies for solar cell technology. *J. Polym. Sci., Part B: Polym. Phys.* **2011**, *49*, 1131.

(3) (a) Martín, N.; Sanchez, L.; Illescas, B.; Pérez, I. C. C_{60}-Based Electroactive Organofullerenes. *Chem. Rev.* **1998**, *98*, 2527. (b) Li, C.-Z.; Yip, H. L.; Jen, A. K.-Y. *J. Mater. Chem.* **2012**, *22*, 4161.

(4) (a) Lucafò, M.; Gerdol, M.; Pallavicini, A.; Pacor, S.; Zorzet, S.; Da Ros, T.; Prato, M.; Sava, G. Profiling the molecular mechanism of fullerene cytotoxicity on tumor cells by RNA-seq. *Toxicology* **2013**, *314*, 183. (b) Lucafò, M.; Pacor, S.; Fabbro, C.; Ros, T.; Zorzet, S.; Prato, M.; Sava, G. Study of a potential drug delivery system based on carbon nanoparticles: effects of fullerene derivatives in MCF7 mammary carcinoma cells. *J. Nanopart. Res.* **2012**, *14*, 830.

(5) (a) Orlova, M. A.; Trofimova, T. P.; Orlov, A. P.; Shatalov, O. A. Perspectives of fullerene derivatives in PDT and radiotherapy of cancers. *Br. J. Med. Med. Res.* **2013**, *3*, 1731. (b) Kharisov, B. I.; Kharissova, O. V.; Gomez, M. J.; Mendez, U. O. Recent Advances in the Synthesis, Characterization, and Applications of Fulleropyrrolidine. *Ind. Eng. Chem. Res.* **2009**, *48*, 545.

(6) Lucafò, M.; Pelillo, C.; Carini, M.; Da Ros, T.; Prato, M.; Sava, G. A Cationic [60] Fullerene Derivative Reduces Invasion and Migration of HT-29 CRC Cells in Vitro at Dose Free of Significant Effects on Cell Survival. *Nano-Micro Lett.* **2014**, *6*, 163.

(7) Mateo-Alonso, A.; Guldi, D. M.; Paolucci, F.; Prato, M. Fullerenes: Multitask Components in Molecular Machinery. *Angew. Chem., Int. Ed.* **2007**, *46*, 8120.

(8) Braun, T. The Epidemic Spread of Fullerene Research. *Angew. Chem., Int. Ed. Engl.* **1992**, *31*, 588.

(9) *Polymers: Chemistry and Physics of Modern Materials*, 3rd ed.; Cowie, J. M. G., Arrighi, V., Eds.; CRC Press: Boca Raton, FL, 2008.

(10) (a) Giacalone, F.; Martín, N. Fullerene polymers: synthesis and properties. *Chem. Rev.* **2006**, *106*, 5136. (b) Main-Chain and Side-Chain C_{60}-Polymers: Giacalone, F.; Martín, N. In *Fullerene Polymers: Synthesis, Properties and Applications*; Martín, N., Giacalone, F., Eds.; Wiley-VCH Verlag GmbH & Co. KGaA: Weinheim, 2009.

DOI: 10.1021/acs.macromol.5b02793
Macromolecules 2016, 49, 1681–1691

(11) Gholamkhass, B.; Peckham, T. J.; Holdcroft, S. Poly(3-hexylthiophene) bearing pendant fullerenes: aggregation vs. self-organization. *Polym. Chem.* **2010**, *1*, 708.
(12) (a) Hiorns, R. C.; Cloutet, E.; Ibarboure, E.; Vignau, L.; Lemaître, N.; Guillerez, S.; Absalon, C.; Cramail, H. Main-Chain Fullerene Polymers for Photovoltaic Devices. *Macromolecules* **2009**, *42*, 3549. (b) Hiorns, R. C.; Cloutet, E.; Ibarboure, E.; Khoukh, A.; Bejbouji, H.; Vignau, L.; Cramail, H. Synthesis of Donor−Acceptor Multiblock Copolymers Incorporating Fullerene Backbone Repeat Units. *Macromolecules* **2010**, *43*, 6033.
(13) Urien, M.; Wantz, G.; Cloutet, E.; Hirsch, L.; Tardy, P.; Vignau, L.; Cramail, H.; Parneix, J.-P. Field-effect transistors based on poly(3-hexylthiophene): Effect of impurities. *Org. Electron.* **2007**, *8* (6), 727.
(14) Gügel, A.; Belik, P.; Walter, M.; Kraus, A.; Harth, E.; Wagner, M.; Spickermann, J.; Müllen, K. The repetitive Diels-Alder reaction: A new approach to [60] fullerene main-chain polymers. *Tetrahedron* **1996**, *52*, 5007.
(15) Shi, S.; Khemani, K. C.; Li, Q. C.; Wudl, F. A polyester and polyurethane of diphenyl C_{61}: retention of fulleroid properties in a polymer. *J. Am. Chem. Soc.* **1992**, *114*, 10656.
(16) Ito, H.; Ishida, Y.; Saigo, K. Regio-and diastereo-controlled synthesis of bis(formylmethano)[60]fullerenes and their application to the formation of [60]fullerene pearl-necklace polyimines. *Tetrahedron Lett.* **2006**, *47*, 3095.
(17) (a) Mishra, A.; Bäuerle, P. Small Molecule Organic Semiconductors on the Move: Promises for Future Solar Energy Technology. *Angew. Chem., Int. Ed.* **2012**, *51*, 2020. (b) Li, Y. *Chem. - Asian J.* **2013**, *8*, 2316. (c) He, Y.; Chen, H.-Y.; Hou, J.; Li, Y. Indene−C_{60} Bisadduct: A New Acceptor for High-Performance Polymer Solar Cells. *J. Am. Chem. Soc.* **2010**, *132*, 1377. (d) Lenes, M.; Wetzelaer, G.-J. A. H.; Kooistra, F. B.; Veenstra, S. C.; Hummelen, K. J.; Blom, P. W. M. *Adv. Mater.* **2008**, *20*, 2116.
(18) Hirsch, A. *The Chemistry of the Fullerenes*; Thieme: Stuttgart, Germany, 1994.
(19) Izquierdo, M.; Cerón, M. R.; Alegret, N.; Metta-Magaña, A. J.; Rodríguez-Fortea, A.; Poblet, J. M.; Echegoyen, L. Unexpected Isomerism in *cis*-2 Bis(pyrrolidino)[60]Fullerene Diastereomers. *Angew. Chem., Int. Ed.* **2013**, *52*, 12928.
(20) Kordatos, K.; Bosi, S.; Da Ros, T.; Zambon, A.; Lucchini, V.; Prato, M. Isolation and Characterization of All Eight Bisadducts of Fulleropyrrolidine Derivatives. *J. Org. Chem.* **2001**, *66*, 2802.
(21) Hiorns, R. C.; Iratçabal, P.; Bégué, D.; Khoukh, A.; de Bettignies, R.; Leroy, J.; Firon, M.; Sentein, C.; Martinez, H.; Preud'homme, H.; Dagron-Lartigau, C. Alternatively linking fullerene and conjugated polymers. *J. Polym. Sci., Part A: Polym. Chem.* **2009**, *47*, 2304.
(22) Santos Silva, H.; Tournebize, A.; Bégué, D.; Peisert, H.; Chassé, T.; Gardette, J.-L.; Thérias, S.; Rivaton, A.; Hiorns, R. C. A universal route to improving conjugated macromolecule photostability. *RSC Adv.* **2014**, *4*, 54919.
(23) Wang, B.; Wasielewski, M. R. Design and Synthesis of Metal Ion-Recognition-Induced Conjugated Polymers: An Approach to Metal Ion Sensory Materials. *J. Am. Chem. Soc.* **1997**, *119*, 12.
(24) van der Made, A. W.; van der Made, R. H. A convenient procedure for bromomethylation of aromatic compounds. Selective mono-, bis-, or trisbromomethylation. *J. Org. Chem.* **1993**, *58*, 1262.
(25) Shao, P.; Li, Z.; Luo, J.; Wang, H.; Qin, J. A Convenient Synthetic Route to 2,5-Dialkoxyterephthalaldehyde. *Synth. Commun.* **2005**, *35*, 49.
(26) Audouin, F.; Nuffer, R.; Mathis, C. Synthesis of di- and tetra-adducts by addition of polystyrene macroradicals onto fullerene C_{60}. *J. Polym. Sci., Part A: Polym. Chem.* **2004**, *42*, 3456.
(27) Jenkins, A. D.; Kratochvíl, P.; Stepto, R. F. T.; Suter, U. W. Glossary of Basic Terms in Polymer Science (IUPAC Recommendations 1996). *Pure Appl. Chem.* **1996**, *68*, 2287.
(28) (a) Pepels, M. P. F.; Souljé, P.; Peters, R.; Duchateau, R. Theoretical and experimental approach to accurately predict the complex molecular weight distribution in the polymerization of strainless cyclic esters. *Macromolecules* **2014**, *47*, 5542. (b) Di Stefano, S. Theoretical features of macrocyclization equilibria and their application on transacetalation based dynamic libraries. *J. Phys. Org. Chem.* **2010**, *23*, 797.
(29) *Gaussian 09, Revision E.01*: Frisch, M. J.; Trucks, G. W.; Schlegel, H. B.; Scuseria, G. E.; Robb, M. A.; Cheeseman, J. R.; Scalmani, G.; Barone, V.; Mennucci, B.; Petersson, G. A.; Nakatsuji, H.; Caricato, M.; Li, X.; Hratchian, H. P.; Izmaylov, A. F.; Bloino, J.; Zheng, G.; Sonnenberg, J. L.; Hada, M.; Ehara, M.; Toyota, K.; Fukuda, R.; Hasegawa, J.; Ishida, M.; Nakajima, T.; Honda, Y.; Kitao, O.; Nakai, H.; Vreven, T.; Montgomery, J. A., Jr.; Peralta, J. E.; Ogliaro, F.; Bearpark, M.; Heyd, J. J.; Brothers, E.; Kudin, K. N.; Staroverov, V. N.; Kobayashi, R.; Normand, J.; Raghavachari, K.; Rendell, A.; Burant, J. C.; Iyengar, S. S.; Tomasi, J.; Cossi, M.; Rega, N.; Millam, J. M.; Klene, M.; Knox, J. E.; Cross, J. B.; Bakken, V.; Adamo, C.; Jaramillo, J.; Gomperts, R.; Stratmann, R. E.; Yazyev, O.; Austin, A. J.; Cammi, R.; Pomelli, C.; Ochterski, J. W.; Martin, R. L.; Morokuma, K.; Zakrzewski, V. G.; Voth, G. A.; Salvador, P.; Dannenberg, J. J.; Dapprich, S.; Daniels, A. D.; Farkas, Ö.; Foresman, J. B.; Ortiz, J. V.; Cioslowski, J.; Fox, D. J. Gaussian, Inc.: Wallingford, CT, 2009. (b) Dewar, M. J. S.; Thiel, W. Ground-States of Molecules. 38. The MNDO Method: Approximations and Parameters. *J. Am. Chem. Soc.* **1977**, *99*, 4899.
(30) Bottari, G.; Dammann, C.; Torres, T.; Drewello, T. Laser-induced azomethine ylide formation and its covalent entrapment by fulleropyrrolidine derivatives during MALDI analysis. *J. Am. Soc. Mass Spectrom.* **2013**, *24*, 1413.
(31) Kordatos, K.; Prato, M.; Menna, E.; Scorrano, G.; Maggini, M. Synthesis of Fullerene Derivatives for Incorporation in Sol-Gel Glasses. *J. Sol-Gel Sci. Technol.* **2001**, *22*, 237.
(32) (a) Stepto, R. F. T.; Gilbter, R. G.; Hess, M.; Jenkins, A. D.; Jones, R. G.; Kratochvíl, P. Dispersity in polymer science (IUPAC Recommendations 2009). *Pure Appl. Chem.* **2009**, *81*, 351. (b) Hiorns, R. C.; Boucher, R. J.; Duhlev, R.; Hellwich, K.-H.; Hodge, P.; Jenkins, A. D.; Jones, R. G.; Kahovec, J.; Moad, G.; Ober, C. K.; Smith, D. W.; Stepto, R. F. T.; Vairon, J.-P.; Vohlídal, J. A Brief Guide to Polymer Nomenclature (IUPAC Technical report). *Pure Appl. Chem.* **2012**, *84*, 2167.
(33) (a) Flory, P. J. *Principles of Polymer Chemistry*; Cornell University Press: Ithaca, NY, 1953; Chapter 8. (b) Flory, P. J. Molecular Size Distribution in Linear Condensation Polymers. *J. Am. Chem. Soc.* **1936**, *58*, 1877.
(34) Odian, G. *Principles of Polymerization*, 4th ed.; John Wiley and Sons Inc.: Hoboken, NJ, 2004; Chapter 2.
(35) (a) Martín, N.; Altable, M.; Filippone, S.; Martín-Domenech, A.; Echegoyen, L.; Cardona, C. M. Retro-Cycloaddition Reaction of Pyrrolidinofullerenes. *Angew. Chem., Int. Ed.* **2006**, *45*, 110. (b) Martín, N.; Altable, M.; Filippone, S.; Martín-Domenech, A. New Reactions in Fullerene Chemistry. *Synlett* **2007**, *2007* (20), 3077. (c) Filippone, S.; Izquierdo Barroso, M.; Martín-Domenech, A.; Osuna, S.; Solà, M.; Martín, N. On the Mechanism of the Thermal Retrocycloaddition of Pyrrolidinofullerenes (Retro-Prato Reaction). *Chem. - Eur. J.* **2008**, *14*, 5198.
(36) Yang, C.; Lee, J. K.; Heeger, A. J.; Wudl, F. Well-defined donor−acceptor rod−coil diblock copolymers based on P3HT containing C_{60}: the morphology and role as a surfactant in bulk-heterojunction solar cells. *J. Mater. Chem.* **2009**, *19*, 5416.
(37) Penn, S. G.; Costa, D. A.; Balch, A. L.; Lebrilla, C. B. Analysis of C_{60} oxides and $C_{120}On$ (n = 1,2,3) using matrix assisted laser desorption-ionization Fourier transform mass spectrometry. *Int. J. Mass Spectrom. Ion Processes* **1997**, *169/170*, 371.
(38) (a) Rao, A. M.; Zhou, P.; Wang, K. A.; Hager, G. T.; Holden, J. M.; Wang, Y.; Lee, W. T.; Bi, X.-X.; Eklund, P. C.; Cornett, D. S. Photoinduced polymerization of solid C_{60} films. *Science* **1993**, *259*, 955. (b) Eklund, P.; Rao, A. M.; Zhou, P.; Wang, Y.; Holden, J. M. Photochemical transformation of C_{60} and C_{70} films. *Thin Solid Films* **1995**, *257*, 185.
(39) (a) Petersson, G. A.; Bennett, A.; Tensfeldt, G. A.; Al-Laham, M. A.; Shirley, W. A.; Mantzaris, J. A complete basis set model chemistry. I. The total energies of closed-shell atoms and hydrides of

DOI: 10.1021/acs.macromol.5b02793
Macromolecules 2016, 49, 1681−1691

the first-row elements. *J. Chem. Phys.* **1988**, *89*, 2193. (b) Becke, A. D. Density-functional thermochemistry. III. The role of exact exchange. *J. Chem. Phys.* **1993**, *98*, 5648. (c) Lee, C.; Yang, W.; Parr, R. G. *Phys. Rev. B: Condens. Matter Mater. Phys.* **1988**, *37*, 785. (d) Voska, S. H.; Wilk, L.; Nusair, M. *Can. J. Phys.* **1980**, *58*, 1200. (d) Stephens, P. J.; Devlin, F. J.; Chabalowski, C. F.; Frisch, M. J. Ab Initio Calculation of Vibrational Absorption and Circular Dichroism Spectra Using Density Functional Force Fields. *J. Phys. Chem.* **1994**, *98*, 11623.

(40) (a) Neese, F.; Wennmohs, F.; Hansen, A.; Becker, U.; Neese, F.; Wennmohs, F.; Hansen, A.; Becker, U. *Chem. Phys.* **2009**, *356*, 98; *Chem. Phys.* **2009**, *356*, 98. (b) Huber, C.; Klamroth, T. Explicitly time-dependent coupled cluster singles doubles calculations of laser-driven many-electron dynamics. *J. Chem. Phys.* **2011**, *134*, 054113.

(41) Marchesan, S.; Da Ros, T.; Prato, M. Isolation and Characterization of Nine Tris-adducts of *N*-Methylfulleropyrrolidine Derivatives. *J. Org. Chem.* **2005**, *70*, 4706.

(42) (a) Sustmann, R. *Pure Appl. Chem.* **1974**, *40*, 569. (b) Sustmann, R. IUPAC Conference on Physcial Organic Chemistry, International Conference on Physical Organic Chemistry, ICPOC, Physical organic Chemistry, Second, Noordwikerhout, The Netherlands, 1974-04-29-1974-05-02.

(43) Hirsh, A.; Lampharth, I.; Karfunkel, H. R. Fullerene Chemistry in Three Dimensions: Isolation of Seven Regioisomeric Bisadducts and Chiral Trisadducts of C_{60} and Di(ethoxycarbonyl)methylene. *Angew. Chem., Int. Ed. Engl.* **1994**, *33*, 437.

(44) Andersson, C.-H.; Berggren, G.; Ott, S.; Grennberg, H. Synthesis and IR Spectroelectrochemical Studies of a [60]-Fulleropyrrolidine-(tricarbonyl)chromium Complex: Probing C60 Redox States by IR Spectroscopy. *Eur. J. Inorg. Chem.* **2011**, *2011*, 1744.

(45) Tanatar, M. A.; Graja, A.; Zhu, D. B.; Li, Y. L. Spectral investigation of a [60]fulleropyrrolidine. *Synth. Met.* **1998**, *94*, 83.

(46) Dang, M. T.; Hirsch, L.; Wantz, G. P3HT:PCBM, Best Seller in Polymer Photovoltaic Research. *Adv. Mater.* **2011**, *23*, 3597.

DOI: 10.1021/acs.macromol.5b02793
Macromolecules 2016, 49, 1681−1691